Frequency Selectivity of 60-GHz LOS and NLOS Indoor Radio Channels

Haibing Yang, Peter F.M. Smulders and Matti H.A.J. Herben
Radio Communications Group (TTE-ECR), Faculty of Electrical Engineering,
Eindhoven University of Technology, P.O. Box 513, 5600 MB Eindhoven, The Netherlands
Email: {H.Yang, P.F.M.Smulders and M.H.A.J.Herben}@tue.nl

Abstract— **This paper analyzes the frequency selectivity, which is caused by multipath effects, of indoor line-of-sight (LOS) and non-LOS (NLOS) channels based on channel measurements in the frequency band of 60 GHz. The coherence bandwidth is determined to characterize frequency selectivity figures of the channels employing the combination of omnidirectional, fan-beam and pencil-beam antennas at transmitter (TX) and receiver (RX) sides. The results quantitatively show how far directional configurations are more effective for combating multipath effect than the omnidirectional ones for LOS channels. The frequency selectivity of the fan-beam-to-fan-beam configuration is less sensitive to misaligned TX-RX beams than the fan-beam-to-pencil-beam one. In addition, when omnidirectional antennas are used at both TX and RX side, the frequency selectivity of a NLOS channel is less sensitive to the TX-RX height difference than that of a LOS channel. Moreover, coherence bandwidth is empirically related to root-mean-squared delay spread. Lastly, the results presented in this paper lead to some useful insights into antenna configurations and beamformer designs for a 60-GHz radio system.**

I. Introduction

With the ever-increasing demand for radio frequency resource, the use of frequency spectrum for the wireless local network (WLAN) system is steadily moving from the congested frequency range ($2 \sim 5$ GHz) to the uncongested frequency range ($57 \sim 66$ GHz). Recently, the IEEE 802.15.3 Task Group 3c was formed to standardize the 60-GHz wireless personal area network (WPAN) systems, which are intended to provide user data rates in excess of 2 Gbps [1]. For indoor applications, the 60-GHz radio system will be probably limited in a single room environment due to severe attenuations by walls and floors [2]. This offers the advantage that the frequency band can be reused in neighboring rooms due to limited co-channel interference.

One of the biggest challenges for designing such a high data rate radio system is the limited link budget due to high path loss during radio propagation [1]–[3]. For a fixed separation between transmitter (TX) and receiver (RX), the propagation loss at 60 GHz is about 30 dB higher than at 2 GHz in free space. In this sense, it is preferable to employ high gain directive antennas, especially for point-to-point applications. Thanks to the relatively small dimensions of 60-GHz antennas, an alternative to high gain antennas is to use highly flexible antenna arrays for adaptive beamforming. On the other side, an omnidirectional antenna might be used in some applications where a full coverage is required. Therefore, designing a radio system at 60 GHz requires good knowledge of how different antenna configurations and antenna pointing errors will influence the channel characteristics.

Coherence bandwidth is a statistical measure for characterizing channel frequency selectivity. If the coherence bandwidth of the channel is less than the transmission bandwidth, complicated techniques, such as coding diversity or equalization, have to be used for helping the recovery of the transmitted signal. Coherence bandwidth figures of 60-GHz radio channels have been reported in [4]–[6]. In these, the coherence bandwidths in corridor environments are found to be highly variable with the RX location with respect to the TX and can vary from several MHz to tens of MHz [4], [5]. For both horn-omni and horn-horn antenna configurations, the results don't show a significant difference [4]. In room or laboratory environments, the coherence bandwidths are quite dependent on the environment and the antenna configuration employed [4], [6].

In this paper, extensive measurements are conducted in indoor line-of-sight (LOS) and non-LOS (NLOS) environments in the frequency band of 60 GHz. The coherence bandwidth is used to quantitatively characterize the frequency selectivity. The impacts of different antenna configurations, including omnidirectional-to-omnidirectional (Omn-Omn), fan-beam-to-omnidirectional (Fan-Omn), fan-beam-to-fan-beam (Fan-Fan) and fan-beam-to-pencil-beam (Fan-Pen) configurations, on frequency selectivity will be analyzed and compared. Next, we analyze the impact of antenna beam pointing error on frequency selectivity. Besides, the coherence bandwidth is empirically related to the root-mean-squared delay spread (RDS) which is highly related to the Rician K-factor. Lastly, the results and analysis presented lead to useful insights into some system design issues of a 60-GHz radio system.

II. Experimental setup and scenarios

A. Experimental setup and antennas used

The employed channel sounding system was built around an HP 8510C vector network analyzer, which is capable of measuring complex frequency response, i.e. S_{21} parameter, of a channel. A detailed description of this system can be found in [2]. During measurement, the step sweep mode was used and the sweep time of each measurement was about 20 seconds [7]. Channel impulse responses were obtained by Fourier transforming the S_{21} parameters into time domain after

0-7803-9392-9/06/$20.00 (c) 2006 IEEE

a Kaiser window was applied with a sidelobe level of -44 dB. The S_{21} parameters were measured in the frequency range of $57 \sim 59$ GHz or $58 \sim 59$ GHz with 401 sample points in two room environments, respectively.

Three types of vertical polarized antennas with different radiative patterns, i.e. omnidirectional, fan-beam and pencil-beam antennas, were applied in our measurements. Parameters of these antennas, half power beamwidth (HPBW) and antenna gain, are listed in Table I.

TABLE I
ANTENNA PARAMETERS

Type of antennas	Half power beamwidth (^{o})		Gain (dBi)
	E-plane	H-plane	
Fan-beam	12.0	70.0	16.5
Pencil-beam	8.3	8.3	24.4
Omnidirectional	9.0	omnidirectional	6.5

B. Indoor environments and TX-RX configurations

Two groups of measurements were conducted in the room A and B, separately, on the 11^{th} floor of the EH-building at Eindhoven University of Technology. The dimensions of the rooms are $11.2 \times 6.0 \times 3.2$ m^3 and $7.2 \times 6.0 \times 3.2$ m^3, respectively. Both rooms have a similar structure. The window side consists of window glasses with a metallic frame one meter above the floor and a metallic heating radiator below the window. The concrete walls are smoothly plastered and the concrete floor is covered with linoleum. The ceiling consists of aluminium plates and light holders. Some large metallic objects, such as cabinets, were standing on the ground. More detailed descriptions of the environments can be found in [8] and [9].

TABLE II
MEASUREMENT SCENARIOS AND CONFIGURATIONS

Room	Freq. range (GHz)	Antenna (TX-RX)			Denoted
		TX	RX	Height (m)	
A†	$57 \sim 59$	Omn.	Omn.	1.4 – 1.4	$OO_{0.0}$
				1.9 – 1.4	$OO_{0.5}$
				2.4 – 1.4	$OO_{1.0}$
B‡	$58 \sim 59$	Fan.	Omn.	2.4 – 1.4	FO
			Fan.		FF, $FF_{\pm 35^o}$
			Pen.		FP, $FP_{\pm 35^o}$

† In room A, the antenna beam is always kept in the horizontal plane.
‡ In room B, the RX beam is elevated towards the TX antenna, except the omnidirectional antenna kept in the horizontal plane.

Table II lists the measurement system configurations and scenarios. In room A, at both the TX and RX side, we use the same type of omnidirectional antennas. Three height differences of TX-RX were considered (denoted by $OO_{0.0}$, $OO_{0.5}$ and $OO_{1.0}$, respectively). Both LOS and NLOS channels were measured in the room A. In room B, a sectoral horn antenna with fan-beam pattern was applied at the TX side and located in a corner of the room at the height of 2.4 m. At the RX side, we used three types of antennas with omnidirectional, fan-beam and pencil-beam patterns at the height of 1.4 m. The TX-RX combinations are denoted by FO, FF and FP, respectively, in which of the latter two cases the TX-RX beams are aligned over the boresight. In addition, we measured the channels for the cases of FF and FP with TX-RX beams misaligned by $\pm 35^o$ over the boresight (denoted by $FF_{\pm 35^o}$ and $FP_{\pm 35^o}$). In the room B, only LOS channels were measured.

During measurement, the TX-RX were kept stationary and there were no movements of persons in the rooms.

III. FREQUENCY SELECTIVITY AND EXPERIMENTAL RESULTS

A. Frequency selectivity

Under the assumption that the 60-GHz channel is wide sense stationary and uncorrelated scattering (WSSUS), a coherence bandwidth can be estimated from the frequency autocorrelation function [2], [10], [11]

$$\phi(\Delta f) = \frac{E\{H^*(f)H(f+\Delta f)\}}{E\{|H(f)|^2\}}, \tag{1}$$

where * is conjugate, $E\{\cdot\}$ stands for expectation and $H(f)$ is a measured complex frequency response of the channel. The coherence bandwidth at correlation level s equals the largest frequency separation over which $|\phi(\Delta f)|$ is not smaller than a level s, i.e.

$$Bc_s = \Delta f|_{|\phi(\Delta f)| \geq s}. \tag{2}$$

In this paper, we accept the coherence bandwidth at the level $s = 0.9$ denoted by $Bc_{0.9}$. The coherence bandwidth is a statistical measure in characterizing the frequency selectivity of a channel and a useful parameter for radio system design. When the bandwidth of the transmitted signal is larger than the coherence bandwidth, the signal will fade in different levels at frequencies and the channel is said to be *frequency selective*. On the other hand, when the signal bandwidth is smaller than the coherence bandwidth, the channel is said to be *frequency nonselective*.

Channel frequency selectivity is due to the impact of multi-path propagation and related to the dispersive property in time domain. For a WSSUS channel, the frequency autocorrelation function and the power delay profile are related through the Fourier transform [2], [10], [11]. A smaller RDS generally implies a reduced frequency selectivity and a larger coherence bandwidth. In addition, the RDS of a Rician channel delay profile is strongly related to the K-factor, which is defined as the ratio between the powers contributed by the dominant path and the scattered paths. Generally speaking, the larger is the K-factor, the smaller is the RDS and thus the smaller is the coherence bandwidth. In literature, coherence bandwidth is approximately modelled to be inversely proportional to RDS with a proportionality constant, which is related to the shape of the power delay profile [4], [10].

For the special case of an exponentially decaying power delay profile, the frequency autocorrelation function can be written as [12]

$$\phi(\Delta f) = \frac{1}{K+1}\left(K + \frac{1}{1+j2\pi\Delta f\sigma_\tau K'}\right), \tag{3}$$

where σ_τ is the RDS and $K' = (K+1)/\sqrt{2K+1}$. Here the RDS and the K-factor are related by $\sigma_\tau \cdot K' = 1/\gamma$ with γ the decay exponent of the decaying part. Therefore, the frequency

TABLE III

THE MEAN VALUES OF K, σ_τ, $Bc_{0.9}$ AND $\sigma_\tau Bc_{0.9}$ FOR DIFFERENT CONFIGURATIONS.

Cases	LOS			NLOS			LOS				
	$OO_{0.0}$	$OO_{0.5}$	$OO_{1.0}$	$OO_{0.0}$	$OO_{0.5}$	$OO_{1.0}$	FO	FF	FP	$FF_{\pm 35^o}$	$FP_{\pm 35^o}$
$E\{K\}$	1.1	0.5	0.3	0.9	1.6	0.7	1.7	12.5	14.5	9.8	2.9
$E\{\sigma_\tau\}$ (ns)	7.3	13.8	20.8	12.9	14.8	21.0	14.6	1.2	1.1	1.4	23.3
$E\{Bc_{0.9}\}$ (MHz)	15.4	5.6	3.0	6.4	6.5	2.6	6.3	51.8	55.6	44.7	3.2
$E\{\sigma_\tau \cdot Bc_{0.9}\}$	0.101	0.073	0.060	0.059	0.053	0.039	0.068	0.060	0.059	0.064	0.064

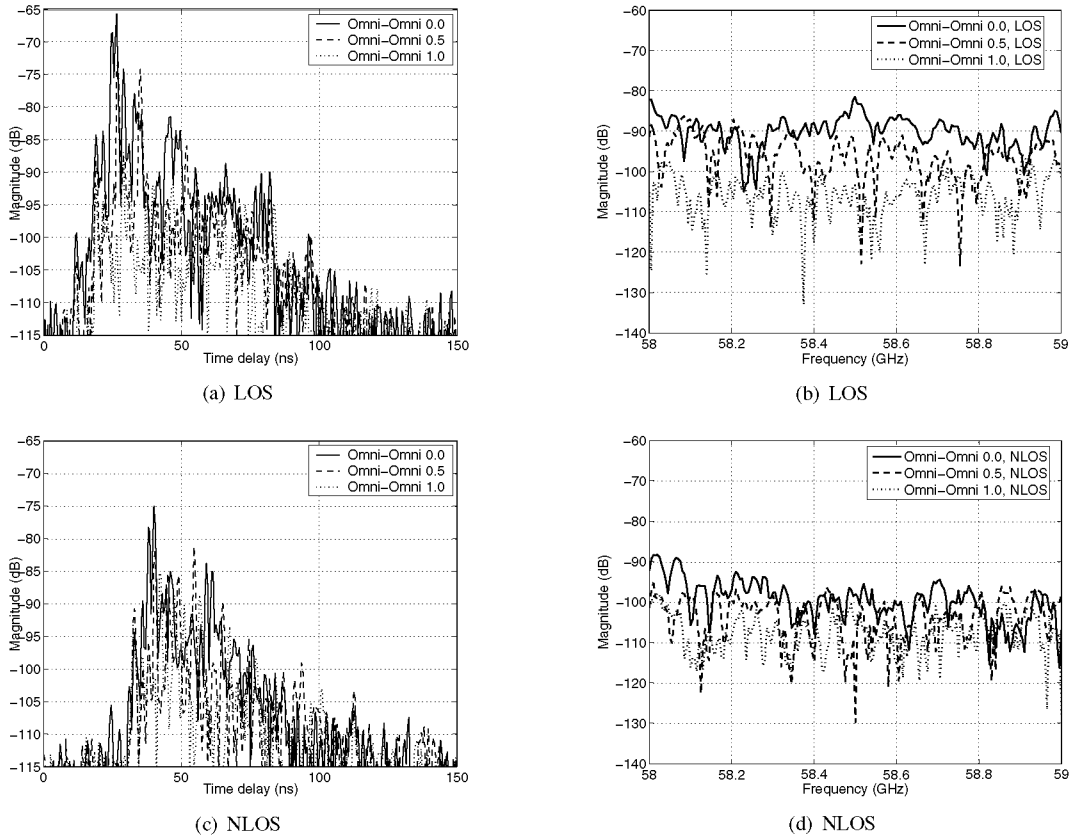

(a) LOS (b) LOS

(c) NLOS (d) NLOS

Fig. 1. Typical channel impulse responses and frequency responses for the Omn-Omn configurations. LOS channel parameters: $K = 0.8, 0.7, 0.2$, $\sigma_\tau = 7.4, 10.1, 24.1$ ns and $Bc_{0.9} = 16.0, 8.0, 2.0$ MHz for three TX heights, respectively; NLOS: $K = 0.7, 0.4, 0.4$, $\sigma_\tau = 9.0, 12.3, 17.7$ ns and $\mathrm{Bc}_{0.9} = 7.0, 6.0, 3.0$ MHz.

autocorrelation function can be uniquely determined by the RDS at a specific decay exponent.

Based on the data sets of channel measurements with different antenna configurations, we investigate the frequency selectivity of 60-GHz channels concerning K-factor, RDS and coherence bandwidth in the following parts. When calculating the K-factor, the power contributed by the dominant path is derived by adding up the powers within the resolution bin. The RDS is calculated from the power delay profile with a dynamic range fixed at 30 dB, which is well above noise level.

B. LOS and NLOS channels with Omn-Omn configurations

Fig.1 depicts the magnitudes of typical channel impulse responses and frequency responses at a position for the Omn-Omn configurations with three TX heights. For the LOS case, when TX/RX antennas are at the same height (i.e. $OO_{0.0}$), some dips in the order of several dBs can be seen in the frequency responses. With the TX height increased ($OO_{0.5}$ and $OO_{1.0}$), the direct path fades and multiple paths arise due to misaligned TX-RX beams [8]. In other words, the K-factor reduces and the RDS becomes larger. As a result, the dip levels become deeper and the dip numbers increase, which is reflected in the reduction of coherence bandwidth. Table III lists the mean values of K-factors, RDSs and coherence bandwidths of all the measured channels for different antenna configurations. For the three Omn-Omn configurations in the LOS case, the mean coherence bandwidths are $Bc_{0.9} = 15.4$, 5.6 and 3.0 MHz, respectively.

For the NLOS channels, the K-factor and the RDS of a NLOS channel become less dependent on the TX-RX height difference but more dependent on the environment, due to the absence of the direct path. The channel characteristics of the case $OO_{0.0}$ in time and frequency gets closer to the case

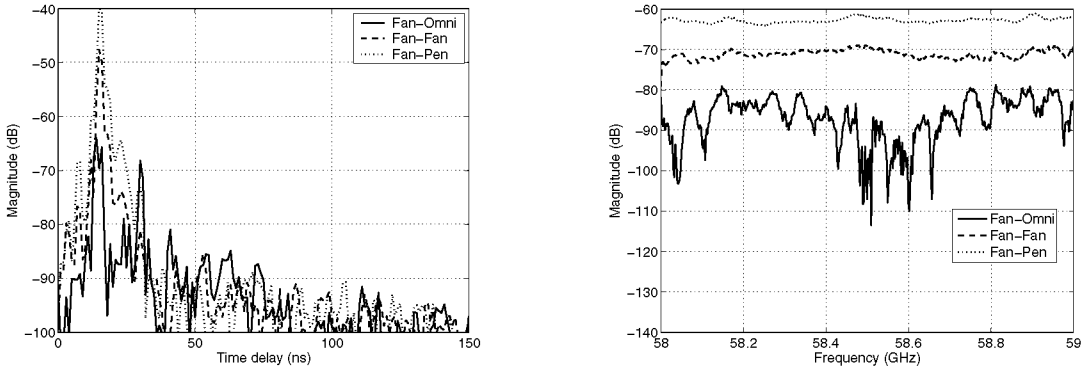

Fig. 2. Typical channel impulse responses (left) and frequency responses (right) of the aligned configurations Fan-Omn, Fan-Fan and Fan-Pen with $K = 1.1, 16.9, 15.7$, $\sigma_\tau = 10.3, 1.0, 1.0$ ns and $Bc_{0.9} = 9.0, 63.0, 65.0$ MHz, respectively.

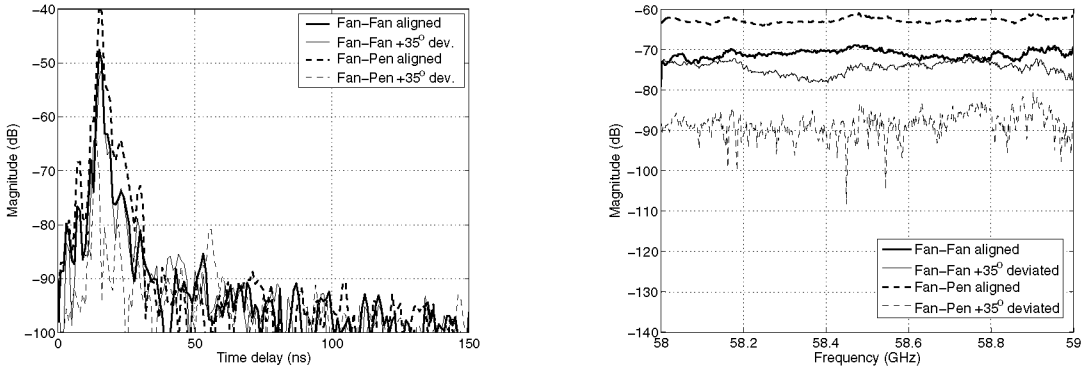

Fig. 3. Typical channel impulse responses (left) and frequency responses (right) of the misaligned configurations Fan-Fan and Fan-Pen with $K = 8.6, 3.8$, $\sigma_\tau = 1.2, 16.1$ ns and $Bc_{0.9} = 60.0, 6.0$ MHz, respectively, compared to the aligned ones in Fig.2.

$OO_{0.5}$, as seen from Fig.1(c) and (d). The average coherence bandwidths of the NLOS channels are $Bc_{0.9} = 6.4$, 6.5 and 2.6 MHz, respectively.

C. LOS channels with the fan-beam antenna at TX side

Fig.2 depicts the typical channel impulse responses and frequency responses of the aligned configurations Fan-Omn, Fan-Fan and Fan-Pen measured at the same position. Clearly, the Fan-Omn configuration shows the severest frequency selectivity with the average $Bc_{0.9} = 6.3$ MHz, which is similar to the Omn-Omn configurations. In contrast, for the channels with Fan-Fan and Fan-Pen configurations, multiple paths are significantly suppressed by the narrow antenna beams as seen from Fig.2, which means large K-factors and small delay spreads. This leads to impressively smooth and almost flat frequency responses. The average coherence bandwidths are 51.8 and 55.6 MHz, respectively, which are considerably larger than the Fan-Omn configuration.

However, the misalignment of the RX beam from the boresight leads to different impacts on the channels with Fan-Fan and Fan-Pen configurations, see Fig.3. For the Fan-Fan one, the deviation of 35^o doesn't cause a noticeable change on the impulse response and frequency response. For the Fan-Pen one, on the contrary, the deviation causes about 25 dB power drop in the direct path and some paths arise in the delay profile. This leads to a fast fluctuation in the frequency response. The average coherence bandwidth of the Fan-Pen one changes from 55.6 MHz, when TX-RX aligned, to 3.2 MHz, when misaligned, while it changes from 51.8 MHz to 44.7 MHz for the Fan-Fan case. Notice that the 35^o-deviation is about half the beamwidth of the fan-beam antenna, which means that the direct path is still within the sight.

D. Coherence bandwidth and RDS

Fig.4 depicts the scatter plot of RDS versus coherence bandwidth $Bc_{0.9}$ for all the measurements. Clearly, the scatter points locate in distinct zones for different configurations. When an omnidirectional antenna is used at either side of TX-RX or both, most of the points stay at the lower-right zone ($Bc_{0.9}$ in $0 \sim 30$ MHz and σ_τ in $5 \sim 40$ ns), while for other configurations with aligned beams they locate in the upper-left zone ($Bc_{0.9}$ in $25 \sim 70$ MHz and σ_τ in $0 \sim 3$ ns). Besides, in the case of a misaligned Fan-Pen case, the scatter points will drop into the lower-right zone, while there is little change for the misaligned Fan-Fan case.

For a Rayleigh fading channel ($K = 0$) with delay profile exponentially decaying, one can obtain $\sigma_\tau \cdot Bc_{0.9} \approx 0.077$ from (2) and (3). Here, we experimentally determine the relationship between $Bc_{0.9}$ and RDS by fitting the scatter points in Fig.4 for all the configurations and get

$$Bc_{0.9}\ (\text{GHz}) = \frac{0.063}{\sigma_\tau(\text{ns})}. \tag{4}$$

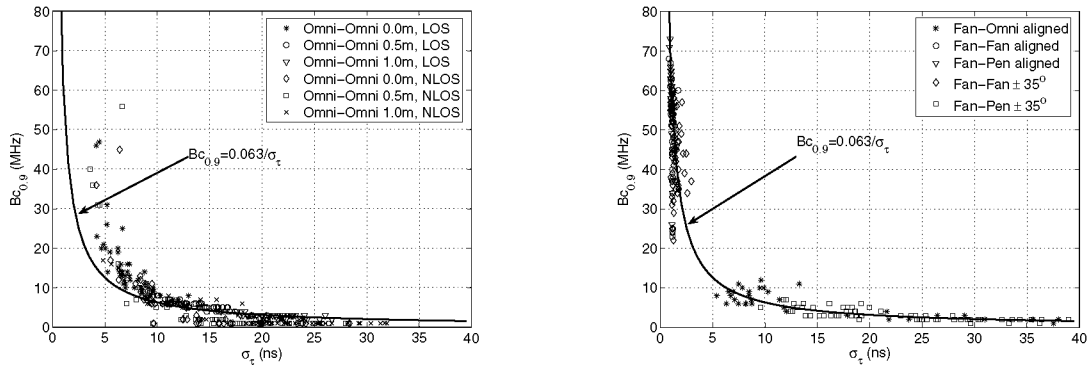

Fig. 4. Scatter plots of correlation bandwidth at 0.9 correlation versus RDS for various antenna configurations.

In comparison, Cox et al. in [10] found $Bc_{0.9} \cdot \sigma_\tau = 0.09$ for outdoor channels at 910 MHz based on extensive measurements.

In addition, Table III lists the mean values of K-factor, σ_τ, $Bc_{0.9}$ and $\sigma_\tau \cdot Bc_{0.9}$ of all the channels for various antenna configurations. If all the power delay profiles have the same shape, one would expect a fixed relationship between coherence bandwidth and RDS [10][12]. Compared with the unified value 0.063 in (4), the distinctions of the mean values of $\sigma_\tau \cdot Bc_{0.9}$ in the table may imply various shapes of power delay profiles for different configurations.

IV. Conclusions

In this paper, we analyzed the frequency selectivity concerning K-factor, RDS and coherence bandwidth based on channel measurements for indoor 60-GHz LOS and NLOS channels. Various antenna configurations were considered. The major conclusions read as follows. First of all, the radiation pattern has a significant impact on the frequency selectivity of a channel. When an omnidirectional antenna was used at TX/RX, coherence bandwidth $Bc_{0.9}$ was below 30 MHz and RDS σ_τ was above 5 ns, while for the directional configurations of Fan-Fan and Fan-Pen, $Bc_{0.9}$ was within $25 \sim 70$ MHz and σ_τ was below 3 ns. For both directional configurations, multiple paths can be significantly suppressed and the frequency responses were quite smooth. However, when TX-RX beams were misaligned, the Fan-Fan configuration was more robust than the Fan-Pen one in the sense of much less impact on the received power and frequency selectivity. In addition, for an Omn-Omn configuration, the frequency selectivity of a LOS channel was quite dependent on the TX-RX height difference, while a NLOS channel shows less dependency. Moreover, for all the antenna configurations together, coherence bandwidths and RDSs were empirically related by $\sigma_\tau \cdot Bc_{0.9} = 0.063$.

Furthermore, the results in this paper lead to some indications for the design of a 60-GHz radio system in an indoor room environment:

- A directional antenna configuration or an adaptive beamformer are effective solutions for combating the frequency selectivity caused by multipath effects. For the beamformer, the beam can be electronically adapted towards the direction of arrival of the strongest path.
- A high gain antenna or beamformer is preferred for a 60-GHz channel, but meanwhile to reduce the impact of the beam's pointing error on the channel, the HPBW has to be properly designed. The coherence bandwidths and RDSs figures presented in this paper have quantitatively determined this impact for some specific pointing errors.

References

[1] IEEE 802.15 WPAN Millimeter Wave Alternative PHY Task Group 3c (TG3c). [Online]. Available: http://www.ieee802.org/15/pub/TG3c.html.

[2] P. Smulders, "Broadband Wireless LANs: A Feasibility Study," Ph.D. dissertation, Einhoven University of Technology, Eindhoven, The Netherlands, Dec. 1995.

[3] ——, "Exploiting the 60 GHz band for local wireless multimedia access: prospects and future directions," *IEEE Commun. Mag.*, vol. 40, pp. 140–147, Jan. 2002.

[4] M. Al-Nuaimi and A. Siamarou, "Coherence bandwidth characterisation and estimation for indoor Rician multipath wireless channels using measurements at 62.4 GHz," *IEE Proceedings: Microwaves, Antennas and Propagation*, vol. 149, no. 3, pp. 181–187, June 2002.

[5] A. Hammoudeh, D. Scammell, and M. Sanchez, "Measurements and Analysis of the Indoor Wideband Millimeter Wave Wireless Radio Channel and Frequency Diversity Characterization," *IEEE Trans. Antennas Propagat.*, vol. 51, no. 10, pp. 2974–2986, Oct. 2003.

[6] A. Pekou, V. Nastos, N. Moraitis, and P. Constantitiou, "Time delay and coherence bandwidth measurements at 60 GHz in an indoor environment for WLANs," in *Proc. IEEE 59th Vehicular Technology Conference (VTC'04-Spring)*, vol. 1, May 2004, pp. 93–97.

[7] Agilent Technologies 8510C Network Analyzer System Operating Manual. May, 2001.

[8] H. Yang, M. Herben, and P. Smulders, "Impact of Antenna Pattern and Reflective Environment on 60 GHz Indoor Radio Channel Characteristics," *IEEE Antennas Wireless Propagat. Lett.*, vol. 4, pp. 300–303, 2005.

[9] J. George, P. Smulders, and M. Herben, "Application of fan-beam antennas for 60GHz indoor wireless communication," *Electronic Letters*, vol. 37, no. 2, pp. 73–74, Jan. 2001.

[10] D. Cox and R. Leck, "Correlation Bandwidth and Delay Spread Multipath Propagation Statistics for 910-MHz Urban Mobile Radio Channels," *IEEE Trans. Wireless Commun.*, vol. 23, pp. 1271–1280, Nov. 1975.

[11] A. Molisch and M. Steinbauer, "Condensed Parameters for Characterizing Wideband Mobile Radio Channels," *International Journal of Wireless Information Networks*, vol. 6, no. 3, pp. 133–154, 1999.

[12] K. Witrisal, "OFDM Air-Interface Design for Multimedia Communications," Ph.D. dissertation, Delft University of Technology, International Research Centre for Telecommunications-transmission and Radar, Oct. 2001.